

## QUANTITATIVE STRUCTURE–RETENTION RELATIONSHIPS ANALYSIS OF RETENTION INDEX OF ESSENTIAL OILS

Hadi Noorizadeh\*, Abbas Farmany and Mehrab Noorizadeh

Department of Chemistry, Faculty of Science, Islamic Azad University, Ilam Branch, Ilam, Iran

Recebido em 7/3/10; aceito em 12/8/10; publicado na web em 30/11/10

Genetic algorithm and multiple linear regression (GA-MLR), partial least square (GA-PLS), kernel PLS (GA-KPLS) and Levenberg-Marquardt artificial neural network (L-M ANN) techniques were used to investigate the correlation between retention index (RI) and descriptors for 116 diverse compounds in essential oils of six *Stachys* species. The correlation coefficient LGO-CV ( $Q^2$ ) between experimental and predicted RI for test set by GA-MLR, GA-PLS, GA-KPLS and L-M ANN was 0.886, 0.912, 0.937 and 0.964, respectively. This is the first research on the QSRR of the essential oil compounds against the RI using the GA-KPLS and L-M ANN.

Keywords: essential oils; genetic algorithm-kernel partial least squares; Levenberg-Marquardt artificial neural network.

### INTRODUCTION

An essential oil is a volatile mixture of organic compounds derived from odorous plant material by physical means.<sup>1</sup> The composition of essential oil has been extensively investigated because of its commercial interest in the fragrance industry (soaps, colognes, perfumes, skin lotion and other cosmetics), in aromatherapy (relaxant), in pharmaceutical preparations for its therapeutic effects as a sedative, spasmolytic, antioxidant, antiviral and antibacterial agent.<sup>2,3</sup> Recently it has also been employed in food manufacturing as natural flavouring for beverages, ice cream, candy, baked goods and chewing gum. *Stachys L.* (*Lamiaceae*, *Lamioideae*) is among the largest genera of *Lamiaceae*. *Stachys* consists of annual and perennial herbs and shrubs showing extensive variation in morphological and cytological characters.<sup>4</sup> *Stachys L.* is a large genus comprising over 300 worldwide species and is widely spread throughout Northern Europe and the Mediterranean.<sup>5</sup> The constituents of essential oil of these spices includes: oxygenated monoterpenes, monoterpene hydrocarbons, oxygenated sesquiterpenes, sesquiterpene hydrocarbons, carbonylic compounds, phenols, fatty acids and esters. These entire compounds have been identified by gas chromatography (GC) and gas chromatography-mass spectrometry (GC-MS). GC and GC-MS are the main methods for identification of these volatile plant oils. To increase the reliability of the MS identification, comprehensive two-dimensional GC-MS can be used. This technique is based on two consecutive GC separations, typically according to boiling point and polarity.<sup>6</sup> The compounds are identified by comparison of retention index with those reported in the literature and by comparison of their mass spectra with libraries or with the published mass spectra data.<sup>7</sup>

Chromatographic retention for capillary column gas chromatography is the calculated quantity, which represents the interaction between stationary liquid phase and gas-phase solute molecule. This interaction can be related to the functional group, electronic and geometrical properties of the molecule.<sup>8,9</sup>

Mathematical modeling of these interactions helps chemists to find a model that can be used to obtain a deep understanding

about the mechanism of interaction and to predict the retention index (RI) of new or even unsynthesized compounds.<sup>10</sup> Building retention prediction models may initiate such theoretical approach, and several possibilities for retention prediction in GC. Among all methods, quantitative structure-retention relationships (QSRR) are most popular. In QSRR, the retention of given chromatographic system was modeled as a function of solute (molecular) descriptors. A number of reports, deals with QSRR retention index calculation of several compounds have been published in the literature.<sup>11-13</sup> The QSRR/QSAR models apply to multiple linear regression (MLR) and partial least squares (PLS) methods often combined with genetic algorithms (GA) for feature selection.<sup>14,15</sup>

Because of the complexity of relationships between the property of molecules and structures, nonlinear models are also used to model the structure–property relationships. Levenberg-Marquardt artificial neural network (L-M ANN) is nonparametric nonlinear modeling technique that has attracted increasing interest. In the recent years, nonlinear kernel-based algorithms as kernel partial least squares (KPLS) have been proposed.<sup>16,17</sup> The basic idea of KPLS is first to map each point in an original data space into a feature space via nonlinear mapping and then to develop a linear PLS model in the mapped space. According to Cover's theorem, nonlinear data structure in the original space is most likely to be linear after high-dimensional nonlinear mapping.<sup>18</sup> Therefore, KPLS can efficiently compute latent variables in the feature space by means of integral operators and nonlinear kernel functions. Compared to other nonlinear methods, the main advantage of the kernel based algorithm is that it does not involve nonlinear optimization. It essentially requires only linear algebra, making it as simple as the conventional linear PLS. In addition, because of its ability to use different kernel functions, KPLS can handle a wide range of nonlinearities. In the present study, GA-MLR, GA-PLS, GA-KPLS and L-MANN were employed to generate QSRR models that correlate the structure of some compound; with observed RI. The present study is a first research on QSRR of the essential oil compounds against the RI, using GA-KPLS and L-M ANN. The performance of these models was compared with those obtained by the GA-MLR and GA-PLS methods.

\*e-mail: hadinoorizadeh@yahoo.com

## EXPERIMENTAL

### Data set

Retention index of essential oils of six *Stachys* species, *S. cretica* L. ssp. *vacillans* Rech. fil., *S. germanica* L., *S. hydrophila* Boiss., *S. nivea* Labill., *S. palustris* L. and *S. spinosa* L., obtained by hydrodistillation, was studied by GC and GC–MS, which contains 116 compounds<sup>19</sup> (Table 1). This set was measured at the same condition with the Innowax column (60 m x 0.25 mm i.d.; 0.33  $\mu$  m film thickness) for GC measurement. GC–MS analysis was also performed on an Agilent 6850 series II apparatus, fitted with a fused silica HP-1 capillary column (30 m x 0.25 mm i.d.; 0.33  $\mu$  m film thickness). The retention index of these compounds was decreased in the range of 3710 and 1075 for both Octadecanoic acid and  $\alpha$ -Pinene, respectively.

In order to evaluate the generated models, we used leave-group-out cross validation (LGO-CV). Cross validation consists of the following: removing one (leave-one-out) or groups (leave-group-out) of compounds in a systematic or random way; generating a model from the remaining compounds, and predicting the removed compounds.

### Descriptor calculation

All structures were drawn with the HyperChem software (version 6). Optimization of molecular structures was carried out by semi-empirical AM1 method using the Fletcher–Reeves algorithm until the root mean square gradient of 0.01 was obtained. Since the calculated values of the electronic features of molecules will be influenced by the related conformation. Some electronic descriptors such as dipole moment, polarizability and orbital energies of LUMO and HOMO were calculated by using the HyperChem software. Also optimized structures were used to calculate 1497 descriptors by DRAGON software version 3.<sup>20</sup>

### Software and programs

A Pentium IV personal computer (CPU at 3.06 GHz) with windows XP operational system was used. Geometry Optimization was performed by HyperChem (version 7.0 Hypercube, Inc.), Dragon software was used to calculate of descriptors. MLR analysis was performed by the SPSS Software (version 13, SPSS, Inc.) by using enter method for model building. Minitab software (version 14, Minitab) was used for the simple PLS analysis. Cross validation, GA-MLR, GA-PLS, GA-KPLS, L-M ANN and other calculation were performed in the MATLAB (Version 7, Mathworks, Inc.) environment.

## THEORY

### Genetic algorithm

Genetic algorithm has been proposed by J. Holland in the early 1970s but it was possible to apply them with reasonable computing times only in the 1990s, when computers became much faster. GA is a stochastic method to solve the optimization problems, defined by fitness criteria applying to the evolution hypothesis of Darwin and different genetic functions, i.e., crossover and mutation.<sup>21</sup> In GA, each individual of the population, defined by a chromosome of binary values as the coding technique, represented a subset of descriptors. The number of genes at each chromosome was equal to the number of descriptors. The population of the first generation was selected randomly. A gene was given the value of one, if its corresponding descriptor was included in the subset; otherwise, it was given the value of zero.<sup>22</sup> The GA performs its optimization by variation and selection via the evaluation of the

**Table 1.** The data set and the corresponding observed and predicted RI values by L-M ANN for the training and test sets

No	Name	RI <sub>Exp</sub>	RI <sub>ANN</sub>	RE <sub>ANN</sub> (%) <sup>a</sup>
Training set				
1	$\alpha$ -Pinene	1075	1064	1.02
2	$\beta$ -Pinene	1118	1110	0.72
3	$\delta$ -Carene	1157	1132	2.16
4	Heptanal	1195	1209	1.17
5	Limonene	1203	1217	1.16
6	$\beta$ -Phellandrene	1218	1216	0.16
7	Ethyl hexanoate	1233	1233	0.00
8	2-Pentylfuran	1244	1257	1.05
9	1-Octen-3-ol	1254	1234	1.59
10	Terpinolene	1265	1257	0.63
11	1-Octen-3-one	1294	1301	0.54
12	(E,E)-2,4-Hexadienal	1395	1363	2.29
13	cis-Linalool	1450	1507	3.93
14	$\alpha$ -Cubebene	1466	1482	1.09
15	$\alpha$ -Copaene	1497	1464	2.20
16	Epi-Bicyclosesquiphellandrene	1498	1521	1.54
17	Pentadecane	1500	1507	0.47
18	Isomenthone	1502	1511	0.60
19	$\beta$ -Bourbonene	1535	1534	0.07
20	$\beta$ -Cubebene	1547	1551	0.26
21	Linalool	1553	1553	0.00
22	$\alpha$ -Longipinene	1579	1562	1.08
23	$\beta$ -Elemene	1598	1583	0.94
24	(E)-Caryophyllene	1612	1620	0.50
25	$\gamma$ -Elemene	1650	1662	0.73
26	(E)-2-Decenal	1655	1652	0.18
27	Pulegone	1662	1656	0.36
28	Phenylacetaldehyde	1663	1660	0.18
29	(Z)-Caryophyllene	1666	1653	0.78
30	cis- $\beta$ -Farnesene	1673	1682	0.54
31	$\alpha$ -Humulene	1689	1697	0.47
32	$\alpha$ -Terpineol	1706	1734	1.64
33	Dodecanol	1709	1716	0.41
34	$\beta$ -Selinene	1715	1713	0.12
35	Borneol	1719	1728	0.52
36	Dodecanal	1724	1720	0.23
37	Germacrene D	1726	1726	0.00
38	$\alpha$ -Muurolole	1740	1761	1.21
39	$\alpha$ -Selinene	1744	1731	0.75
40	Bicyclogermacrene	1756	1740	0.91
41	(E,E)- $\alpha$ -Farnesene	1760	1746	0.80
42	$\delta$ -Cadinene	1773	1786	0.73
43	$\gamma$ -Cadinene	1776	1791	0.84
44	ar-Curcumene	1784	1785	0.06

a: Relative error

**Table 1.** Continuation

No	Name	RI <sub>Exp</sub>	RI <sub>ANN</sub>	RE <sub>ANN</sub> (%) <sup>a</sup>
Training set				
45	(E)-β-Damascenone	1787	1771	0.90
46	Methyl salicylate	1798	1807	0.50
47	Cuparene	1822	1837	0.82
48	(E,E)-2,4-Decadienal	1827	1854	1.48
49	Calamenene	1839	1852	0.71
50	p-Cymen-8-ol	1856	1867	0.59
51	Geraniol	1857	1860	0.16
52	(E)-2-Dodecenal	1868	1882	0.75
53	Benzyl alcohol	1893	1850	2.27
54	2-Phenyl ethyl alcohol	1925	1901	1.25
55	Tetradecanal	1935	1907	1.45
56	β-Ionone	1958	1969	0.56
57	Caryophyllene	2008	2034	1.29
58	Methyl cinnamate	2050	2078	1.37
59	α-Copaen-8-ol	2076	2093	0.82
60	Octanoic	2088	2051	1.77
61	Globulol	2098	2071	1.29
62	Methyl pentadecanoate	2099	2099	0.00
63	Heneicosane	2100	2117	0.81
64	Viridiflorol	2104	2114	0.48
65	Guaiol	2108	2110	0.09
66	α-Cedrol	2120	2109	0.52
67	Hexahydrofamesyl acetone	2131	2114	0.80
68	Cedrenol	2133	2131	0.09
69	Spathulenol	2150	2162	0.56
70	τ-Cadinol	2158	2172	0.65
71	Eugenol	2186	2203	0.78
72	Nonanoic	2190	2227	1.69
73	Thymol	2198	2217	0.86
74	Methyl hexadecanoate	2208	2214	0.27
75	τ-Murolol	2209	2245	1.63
76	α-Bisabolol	2219	2204	0.68
77	α-Cadinol	2255	2218	1.64
78	Decanoic	2298	2254	1.91
79	Caryophylladienol	2316	2349	1.42
80	Dihydroactinidiolide	2354	2368	0.59
81	Indole	2471	2564	3.76
82	Dodecanoic	2503	2580	3.08
83	Benzophenone	2512	2549	1.47
84	(Z)-Phytol	2622	2504	4.50
85	(E)-Phytol	2625	2654	1.10
86	Tetradecanoic acid	2713	2792	2.91
87	Phenanthrene	2814	2907	3.30
88	Pentadecanoic acid	2822	2837	0.53
89	Heptadecanoic acid	2975	2856	4.00

a: Relative error

**Table 1.** Continuation

No	Name	RI <sub>Exp</sub>	RI <sub>ANN</sub>	RE <sub>ANN</sub> (%) <sup>a</sup>
Training set				
90	(Z)-9-Octadecenoic acid	3157	3009	4.69
91	(Z,Z,Z)-9,12,15-Octadecatrienoic acid	3193	3017	5.51
92	Octadecanoic acid	3402	3115	8.44
Test set				
93	Sabinene	1132	1110	1.94
94	(E)-2-Hexenal	1209	1134	6.20
95	p-Cymene	1278	1192	6.73
96	α-Ylangene	1493	1586	6.23
97	(E,E)-2,4-Heptadienal	1506	1537	2.06
98	Benzaldehyde	1541	1541	0.00
99	4-Terpineol	1611	1670	3.66
100	Acetophenone	1657	1659	0.12
101	γ-Murolene	1704	1753	2.88
102	trans-Sabinol	1721	1704	0.99
103	β-Bisabolene	1743	1722	1.20
104	Naphthalene	1763	1763	0.00
105	p-Methoxyacetophenone	1797	1836	2.17
106	(Z)-b-Damascenone	1835	1874	2.13
107	α-Calacorene	1918	1982	3.34
108	(E)-Nerolidol	2050	2144	4.59
109	β-Oplopenone	2098	2062	1.72
110	4-Vinylguaiaicol	2180	2085	4.36
111	Carvacrol	2239	2157	3.66
112	Cadalene	2256	2292	1.60
113	13-epi-Manoyl oxide	2380	2507	5.34
114	Benzyl benzoate	2655	2894	9.00
115	Hexadecanoic acid	2931	3216	9.72
116	(Z,Z)-9,12-Octadecadienoic acid	3157	3032	3.96

a: Relative error

fitness function  $\eta$ . Fitness function was used to evaluate alternative descriptor subsets that were finally ordered according to the predictive performance of related model by cross validation. The fitness function was proposed by Depczynski *et al.*<sup>23</sup> The root-mean-square errors of calibration (RMSEC) and prediction (RMSEP) were calculated and the fitness function was calculated by Equation 1.

$$\mu = \{[(m_c - n - 1) RMSEC^2 + m_p RMSEP^2] / (m_c + m_p - n - 1)\}^{1/2} \quad (1)$$

where  $m_c$  and  $m_p$  are the number of compounds in the calibration and prediction set and  $n$  represent the number of selected variables, respectively. The parameter algorithm reported in Table 2.

### Linear models

#### Multiple linear regression

A major step in constructing the QSRR model is finding a set of molecular descriptors that represent variation in the structural property of the molecules. The modeling and prediction of the physicochemical properties of organic compounds is an important objective in many

**Table 2.** Parameters of the genetic algorithm

Population size: 30 chromosomes
On average, five variables per chromosome in the original population
Regression method: MLR, PLS, KPLS
Cross validation: leave-group-out
Number subset: 4
Maximum number of variables selected in the same chromosome: (MLR, 10), (PLS, 30)
Elitism: True
Crossover: multi Point
Probability of crossover: 50%
Mutation: multi Point
Probability of mutation: 1%
Maximum number of components: (PLS, 10)
Number of runs: 100

scientific fields.<sup>24,25</sup> MLR is one of the most modeling methods in QSRR. MLR method provides an equation that links the structural features to the RI of the compounds:

$$RI = a_0 + a_1 \mathbf{d}_1 + \dots + a_n \mathbf{d}_n \quad (2)$$

where  $a_0$  and  $a_i$  are intercept and regression coefficients of the descriptors, respectively.  $\mathbf{d}_i$  has the common definition, variable or descriptor in this case, the elements of this vector are equivalent numerical values of descriptors of the molecules.

#### Partial least squares

PLS is a linear multivariate method for relating the process variables  $X$  with responses  $Y$ . PLS can analyze data with strongly collinear, noisy, and numerous variables in both  $X$  and  $Y$ .<sup>26</sup> PLS reduces the dimension of the predictor variables by extracting factors or latent variables that are correlated with  $Y$  while capturing a large amount of the variations in  $X$ . This means that PLS maximizes the covariance between matrices  $X$  and  $Y$ . In PLS, the scaled matrices  $X$  and  $Y$  are decomposed into score vectors ( $t$  and  $u$ ), loading vectors ( $p$  and  $q$ ), and residual error matrices ( $E$  and  $F$ ):

$$\begin{aligned} X &= \sum_{i=1}^a t_i p_i^T + E \\ Y &= \sum_{i=1}^a u_i q_i^T + F \end{aligned} \quad (3)$$

where  $a$  is the number of latent variables. In an inner relation, the score vector  $t$  is linearly regressed against the score vector  $u$ .

$$U_i = b_i t_i + h_i \quad (4)$$

where  $b$  is regression coefficient that is determined by minimizing the residual  $h$ . It is crucial to determine the optimal number of latent variables and cross validation is a practical and reliable way to test the predictive significance of each PLS component. There are several algorithms to calculate the PLS model parameters. In this work, the NIPALS algorithm was used with the exchange of scores.<sup>27</sup>

#### Nonlinear

##### Kernel partial least squares

The KPLS method is based on the mapping of the original input

data into a high dimensional feature space  $\mathfrak{S}$  where a linear PLS model is created. By nonlinear mapping  $\Phi: x \in \mathfrak{R}^n - \Phi(x) \in \mathfrak{S}$ , a KPLS algorithm can be derived from a sequence of NIPALS steps and has the following formulation:<sup>28</sup>

1. Initialize score vector  $w$  as equal to any column of  $Y$ .
2. Calculate scores  $u = \Phi \Phi^T w$  and normalize  $u$  to  $\|u\| = 1$ , where  $\Phi$  is a matrix of regressors.
3. Regress columns of  $Y$  on  $u$ :  $c = Y^T u$ , where  $c$  is a weight vector.
4. Calculate a new score vector  $w$  for  $Y$ :  $w = Yc$  and then normalize  $w$  to  $\|w\|=1$ .
5. Repeat steps 2–4 until convergence of  $w$ .
6. Deflate  $\Phi \Phi^T$  and  $Y$  matrices:

$$\Phi \Phi^T = (\Phi - uu^T \Phi)(\Phi - uu^T \Phi)^T \quad (5)$$

$$Y = Y - uu^T Y \quad (6)$$

7. Go to step 1 to calculate the next latent variable.

Without explicitly mapping into the high-dimensional feature space, a kernel function can be used to compute the dot products as follows:

$$k(x_p, x_j) = \Phi(x_p)^T \Phi(x_j) \quad (7)$$

$\Phi \Phi^T$  represents the  $(n \times n)$  kernel Gram matrix  $K$  of the cross dot products between all mapped input data points  $\Phi(x_i), i = 1, \dots, n$ . The deflation of the  $\Phi \Phi^T = K$  matrix after extraction of the  $u$  components is given by:

$$K = (I - uu^T)K(I - uu^T) \quad (8)$$

where  $I$  is an  $m$ -dimensional identity matrix. Taking into account the normalized scores  $u$  of the prediction of KPLS model on training data  $Y$  is defined as:

$$\hat{Y} = KW(U^T KW)^{-1}U^T Y = UU^T Y \quad (9)$$

For predictions on new observation data  $\hat{Y}_i$ , the regression can be written as:

$$\hat{Y}_i = K_i W(U^T KW)^{-1}U^T Y \quad (10)$$

where  $K_i$  is the test matrix whose elements are  $K_{ij} = K(x_i, x_j)$  where  $x_i$  and  $x_j$  present the test and training data points, respectively.

#### Artificial neural network

An artificial neural network (ANN) with a layered structure is a mathematical system that stimulates the biological neural network; consist of computing units named neurons and connections between neurons named synapses.<sup>29,31</sup> Input or independent variables are considered as neurons of input layer, while dependent or output variables are considered as output neurons. Synapses connect input neurons to hidden neurons and hidden neurons to output neurons. The strength of the synapse from neuron  $i$  to neuron  $j$  is determined by mean of a weight,  $W_{ij}$ . In addition, each neuron  $j$  from the hidden layer, and eventually the output neuron, are associated with a real value  $b_j$ , named the neuron's bias and with a nonlinear function, named the transfer or activation function. Because the artificial neural networks (ANNs) are not restricted to linear correlations, they can be used for nonlinear phenomena or curved manifolds.<sup>29</sup> Back propagation neural networks (BNNs) are most often used in analytical applications.<sup>30</sup> The back propagation network receives a set of inputs, which is multiplied by

each node and then a nonlinear transfer function is applied. The goal of training the network is to change the weight between the layers in a direction to minimize the output errors. The changes in values of weights can be obtained using Equation 11:

$$\Delta W_{ij,n} = F_n + \alpha \Delta W_{ij,n-1} \quad (11)$$

where  $\Delta W_{ij,n}$  is the change in the weight factor for each network node,  $\alpha$  is the momentum factor, and  $F$  is a weight update function, which indicates how weights are changed during the learning process. There is no single best weight update function which can be applied to all nonlinear optimizations. One needs to choose a weight update function based on the characteristics of the problem and the data set of interest. Various types of algorithms have been found to be effective for most practical purposes such as Levenberg-Marquardt (L-M) algorithm.

### Levenberg-Marquardt algorithm

While basic back propagation is the steepest descent algorithm, the Levenberg-Marquardt algorithm<sup>32</sup> is an alternative to the conjugate methods for second derivative optimization. In this algorithm, the update function,  $F_n$ , can be calculated using Equations 12 and 13:

$$F_0 = -g_0 \quad (12)$$

$$F_n = -[J^T \times J + \mu I]^{-1} \times J^T \times e \quad (13)$$

where  $J$  is the Jacobian matrix,  $\mu$  is a constant,  $I$  is a identity matrix, and  $e$  is an error function.<sup>33</sup>

## RESULTS AND DISCUSSION

### Linear models

#### GA-MLR analysis

To reduce the original pool of descriptors to an appropriate size, the objective descriptor reduction was performed using various criteria. Reducing the pool of descriptors eliminates those descriptors which contribute either no information or whose information content is redundant with other descriptors present in the pool. From the variable pairs with  $R > 0.90$ , only one of them was used in the modeling, while the variables over 90% and equal to zero or identical were eliminated. With the use of these criteria, 1014 out of 1497 original descriptors were eliminated and remaining descriptors were employed to generate the models with the GA-MLR program. In order to minimize the information overlap in descriptors and to reduce the number of descriptors required in regression equation, the concept of non-redundant descriptors was used in our study. The best equation is selected on the basis of the highest multiple correlation coefficient leave-group-out cross validation (LGO-CV) ( $Q^2$ ), the least RMSECV and relative error of prediction and simplicity of the model. These parameters are probably the most popular measure of how well a regression model fits the data. Among the models proposed by GA-MLR, one model had the highest statistical quality and was repeated more than the others. This model had five molecular descriptors including constitutional descriptors (sum of atomic van der Waals volumes (scaled on Carbon atom)) (Sv), topological descriptors (mean topological charge index of order 1) (JGI1), atom-centred fragments (H attached to C0 ( $sp^3$ ) no X attached to next C) (H-046) and electronic descriptors (dipole moment ( $\mu$ ) and highest occupied molecular orbital (HOMO)). The best QSRR model obtained is given below together with the statistical parameters of the regression in Equation 14.

$$RI = 254.54 (\pm 89.570) + 94 (\pm 16.905 Sv) - 889.068 (\pm 385.064 JGI1) - 45.493 (\pm 9.627 H-046) + 60.559 (\pm 27.924\mu) - 70.717 (\pm 21.384 HOMO) \quad (14)$$

Since mean topological charge index of order 1 coefficient is bigger in the equation, it is very important descriptor compared to the other descriptors in the model. The JGI1, H-046 and HOMO displays a negative sign which indicates that when these descriptors increase the RI decreases. The Sv and  $\mu$  displays a positive sign which indicates that the RI is directly related to these descriptors. The predicted values of RI are plotted against the experimental values for training and test sets in Figure 1a. The statistical parameters of this model, constructed by the selected descriptors, are depicted in Table 3.

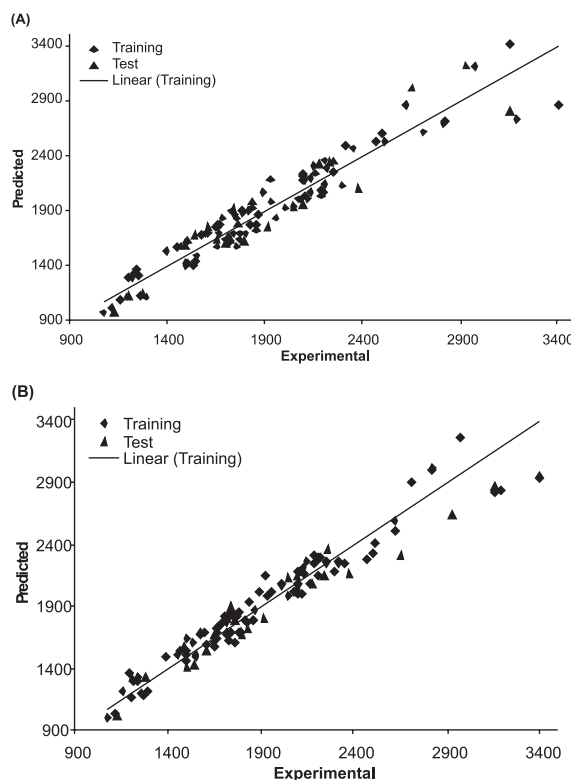


**Figure 1.** Plots of predicted retention index against the experimental values by (a) GA-MLR and (b) GA-PLS models

**Table 3.** The statistical parameters of different constructed QSRR models

Model	Training set					Test set				
	R <sup>2</sup>	Q <sup>2</sup>	RE	RMSE	N	R <sup>2</sup>	Q <sup>2</sup>	RE	RMSE	N
GA-MLR	0.913	0.913	1.91	68.02	92	0.895	0.886	4.12	110.36	24
GA-PLS	0.929	0.924	1.66	61.84	92	0.904	0.912	3.89	107.65	24
GA-KPLS	0.941	0.941	1.38	57.09	92	0.937	0.937	3.88	106.84	24
L-M ANN	0.986	0.983	1.23	49.47	92	0.968	0.964	3.48	98.77	24

#### GA-PLS analysis

The colinearity problem of the MLR method has been overcome through the development of the partial least-squares projections to latent structures (PLS) method. For this reason, after eliminating descriptors that had identical or zero values for greater than 90% of the compounds, 1097 descriptors were remained. These descriptors were employed to generate the models with the GA-PLS and GA-KPLS program. The best PLS model contains 7 selected descriptors in 3

latent variables space. These descriptors were obtained constitutional descriptors (number of rings) (nCIC), topological descriptors (Balaban centric index) (BAC), 2D autocorrelations (Broto-Moreau autocorrelation of a topological structure - lag 5/weighted by atomic masses) (AT5m), geometrical descriptors ((3D-Balaban index) (J3D), RDF descriptors (Radial Distribution Function - 5.5/weighted by atomic van der Waals volumes) (RDF055v), functional group (number of terminal C(sp)) (nR#CH/X) and electronic descriptors (polarizability). For this in general, the number of components (latent variables) is less than the number of independent variables in PLS analysis. The Figure 1b shows the plot of predicted versus experimental values for training and test sets. The obtained statistic parameters of the GA-PLS model were shown in Table 3. The data confirm that higher correlation coefficient and lower prediction error have been obtained by PLS in relative to MLR and these reveal that PLS method produces more accurate results than that of MLR. The PLS model uses higher number of descriptors that allow the model to extract better structural information from descriptors to result in a lower prediction error.

### Nonlinear models

#### GA-KPLS analysis

The leave-group-out cross validation (LGO-CV) has been performed. The  $n$  selected descriptors in each chromosome were evaluated by fitness function of PLS and KPLS based on the Equation 1. In this paper a radial basis kernel function,  $k(x,y) = \exp(-\|x-y\|^2/c)$ , was selected as the kernel function with  $c = m\sigma^2$  where  $r$  is a constant that can be determined by considering the process to be predicted (here  $r$  set to be 1),  $m$  is the dimension of the input space and  $\sigma^2$  is the variance of the data.<sup>34</sup> It means that the value of  $c$  depends on the system under the study. Figure 2a shows the plot of  $Q^2$  versus latent variable for this model. The 5 descriptors in 2 latent variables space chosen by GA-KPLS feature selection methods were contained. These descriptors were obtained constitutional descriptors (number of bonds) (nBT), geometrical descriptors (span R) (SPAN), atom-centred fragments ((phenol/enol/carboxyl OH) and electronic descriptors (lowest unoccupied molecular orbital (LUMO) and polarizability. The Figure 2b shows the plot of predicted versus experimental values for training and test sets. High correlation coefficient and closeness of slope to 1 in the GA-KPLS model reveal a satisfactory agreement between the predicted and the experimental values. For the constructed model, four general statistical parameters were selected to evaluate the prediction ability of the model for the RI. Table 3 shows the statistical parameters for the compounds obtained by applying models to training and test sets. The statistical parameters correlation coefficient ( $R^2$ ), correlation coefficient LGO-CV ( $Q^2$ ), relative error (REP)% and root mean squares error (RMSE) was obtained for proposed models. Each of the statistical parameters mentioned above were used for assessing the statistical significance of the QSRR model. The data presented in Table 3 indicate that the GA-PLS and GA-MLR linear model have good statistical quality with low prediction error, while the corresponding errors obtained by the GA-KPLS model are lower. In comparison with the results obtained by these models suggest that GA-KPLS hold promise for applications in choosing of variable for L-M ANN systems. This result indicates that the RI of essential oils possesses some nonlinear characteristics.

#### Description of some models descriptors

In the chromatographic retention of compounds in the nonpolar or low polarity stationary phases two important types of interactions contribute to the chromatographic retention of the compounds: the induction and dispersion forces. The dispersion forces are related to

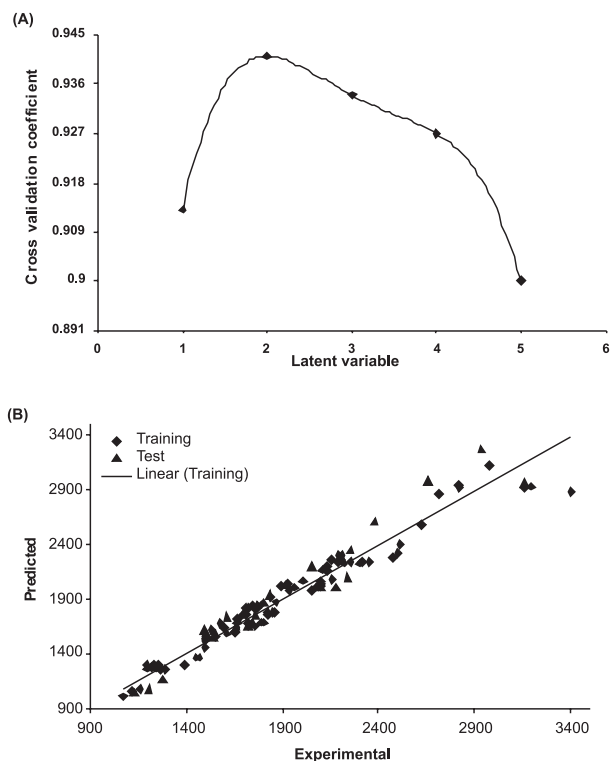


**Figure 2.** Plots of (a) cross validation coefficient obtained by GA-KPLS vs. latent variable and (b) predicted retention index against the experimental values

steric factors, molecular size and branching, while the induced forces are related to the dipolar moment, which should stimulate dipole-induced dipole interactions. For this reason, constitutional descriptors, atom-centred fragments, functional groups and electronic descriptors are very important.

Constitutional descriptors are most simple and commonly used descriptors, reflecting the molecular composition of a compound without any information about its molecular geometry. The most common Constitutional descriptors are number of atoms, number of bond, absolute and relative numbers of specific atom type, absolute and relative numbers of single, double, triple, and aromatic bond, number of ring, number of ring divided by the number of atoms or bonds, number of benzene ring, number of benzene ring divided by the number of atom, molecular weight and average molecular weight.

Electronic descriptors were defined in terms of atomic charges and used to describe electronic aspects both of the whole molecule and of particular regions, such atoms, bonds, and molecular fragments. This descriptor calculated by computational chemistry and therefore can be consider among quantum chemical descriptor. The eigenvalues of LUMO and HOMO and their energy gap reflect the chemical activity of the molecule. LUMO as an electron acceptor represents the ability to obtain an electron, while HOMO as an electron donor represents the ability to donate an electron. The HOMO energy plays a very important role in the nucleophilic behavior and it represents molecular reactivity as a nucleophile. Good nucleophiles are those where the electron residue is high lying orbital. The energy of the LUMO is directly related to the electron affinity and characterizes the susceptibility of the molecule toward attack by nucleophiles. Electron affinity was also shown to greatly influence the chemical behaviour of compounds, as demonstrated by its inclusion in the QSPR/QSRR.<sup>35,36</sup>

The geometrical descriptors which use the modeled three-dimensional coordinates. These descriptors attempt to describe the geometrical environments of carbon atoms. They are usually employed only in situations in which locked conformations are being studied.<sup>37</sup>

Topological descriptors are based on a graph representation of the molecule. They are numerical quantifiers of molecular topology obtained by the application of algebraic operators to matrices representing molecular graphs and whose values are independent of vertex numbering or labeling. They can be sensitive to one or more structural features of the molecule such as size, shape, symmetry, branching and cyclicity and can also encode chemical information concerning atom type and bond multiplicity. Balaban index is a variant of connectivity index, represents extended connectivity and is a good descriptor for the shape of the molecules and modifying biological process. Nevertheless, some of chemists have used this index successfully in developing QSPR/QSRR models.

The radial distribution function descriptors are based on the distances distribution in the geometrical representation of a molecule and constitute a radial distribution function code. Formally, the radial distribution function of an ensemble of  $N$  atoms can be interpreted as the probability distribution of finding an atom in a spherical volume of radius  $r$ .<sup>38</sup>

### L-M ANN analysis

With the aim of improving the predictive performance of nonlinear QSRR model, L-M ANN modeling was performed. Descriptors of GA-KPLS model were selected as inputs in L-M ANN model. The network architecture consisted of five neurons in the input layer corresponding to the five mentioned descriptors. The output layer had one neuron that predicts the RI. The number of neurons in the hidden layer is unknown and needs to be optimized. In addition to the number of neurons in the hidden layer, the learning rate, the momentum and the number of iterations also should be optimized. In this work, the number of neurons in the hidden layer and other parameters except the number of iterations were simultaneously optimized. A Matlab program was written to change the number of neurons in the hidden layer from 2 to 7, the learning rate from 0.001 to 0.1 with a step of 0.001 and the momentum from 0.1 to 0.99 with a step of 0.01. The root mean square errors for training set were calculated for all of the possible combination of values for the mentioned variables in cross validation. It was realized that the RMSE for the training set are minimum when three neurons were selected in the hidden layer and the learning rate and the momentum values were 0.5 and 0.2, respectively. Finally, the number of iterations was optimized with the optimum values for the variables. It was realized that after 13 iterations, the RMSE for prediction set were minimum. The statistical parameters for L-M ANN model in Table 3. Plots of predicted RI versus experimental RI values by L-M ANN are shown in Figure 3. Obviously, there is a close agreement between the experimental and predicted RI and the data represent a very low scattering around a straight line with respective slope and intercept close to one and zero. The closeness of the data to the straight line with a slope equal to 1 shows the perfect fit of the data to a nonlinear model. It should be noted that the data shown in Figure 3 are the predicted values according to leave-group-out cross-validation and a deviation from the regression line is expected for some points. The  $Q^2$ , which is a measure of the model fit to the cross validation set, can be calculated as:

$$R_{cv}^2 \equiv Q^2 = 1 - \frac{\sum_{i=1}^n (y_i - \hat{y}_i)^2}{\sum_{i=1}^n (y_i - \bar{y})^2} \quad (15)$$

where  $y_i$ ,  $\hat{y}_i$  and  $\bar{y}$  were respectively the experimental, predicted, and mean RI values of the samples. The accuracy of cross validation results is extensively accepted in the literature considering the  $Q^2$  value.

In this sense, a high value of the statistical characteristic ( $Q^2 > 0.5$ ) is considered as proof of the high predictive ability of the model.<sup>39</sup> However, several authors suggest that a high value of  $Q^2$  appears to be a necessary but not sufficient condition for a model to have a high predictive power and consider that the predictive ability of a model can only be estimated using a sufficiently large collection of compounds that was not used for building the model.<sup>40</sup>

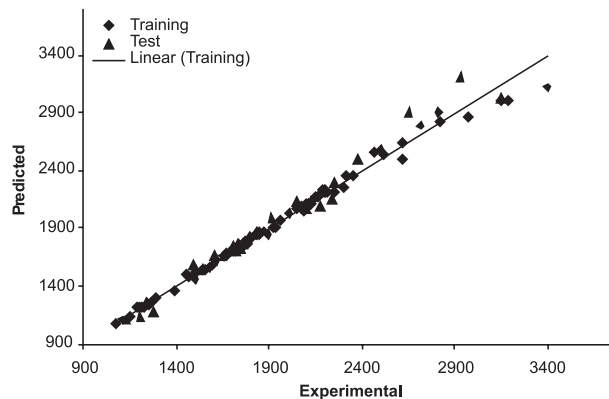


Figure 3. Agreement between predicted RI values and experimental values by L-M ANN

We believe that applying only LGO-CV is not sufficient to evaluate the predictive ability of a model. Thus we employed a two-step validation protocol which contains internal (LGO-CV) and external (test set) validation methods. The data set was randomly divided into training (calibration and prediction sets) and test sets after sorting based on the RI values. The training set consisted of 92 molecules and the test set, consisted of 24 molecules. The training set was used for model development, while the test set in which its molecules have no role in model building was used for evaluating the predictive ability of the models for external set. We reported that the retention index of this essential oil was mainly controlled by constitutional descriptors, functional groups and electronic descriptors.

The statistical parameters obtained by LGO-CV for L-M ANN, GA-KPLS and the linear QSRR models are compared in Table 3. Inspections of the results of this table reveals a higher  $R^2$  and  $Q^2$  values and lower the RE for L-M ANN model for the training and test sets compared with their counterparts for GA-KPLS and other models. Moreover, the low values of root-mean-square error of prediction for the samples in the test set confirm the prediction ability of the resulted models for the compounds that were not used in the model-building step. In comparison with the plot of other models, the L-M ANN predicted RI of each one of the training and test sets compound represent a uniform and linear distribution. This clearly shows the strength of L-M ANN as a nonlinear feature selection method. The key strength of L-M ANN is their ability to allow for flexible mapping of the selected features by manipulating their functional dependence implicitly. Neural network handles both linear and nonlinear relationship without adding complexity to the model. This capacity offset the large computing time required and complexity of L-M ANN model with respect other models.

### CONCLUSION

The essential oils are widely used in pharmaceutical, cosmetic and perfume industry, and for flavouring and preservation of several food products. GC and GC-MS is one of the most powerful tools in analytical volatile compound (such as essential oils). In this study, an accurate QSRR model for estimating the retention index (RI) of essential oils of six *Stachys* species which obtained by GC and GC-MS

was developed by employing the two linear models (GA-MLR and GA-PLS) and two nonlinear models (GA-KPLS and L-M ANN). The most important molecular descriptors selected represent the constitutional descriptors, functional group and electronic descriptors that are known to be important in the retention mechanism of essential oils. Four models have good predictive capacity and excellent statistical parameters. A comparison between these models revealed the superiority of the GA-KPLS and L-M ANN to other models. It is easy to notice that there was a good prospect for the GA-KPLS and L-M ANN application in the QSRR modeling. This indicates that the RI of essential oils possesses some nonlinear characteristics. In comparison with two nonlinear models, the results showed that the L-M ANN model can be effectively used to describe the molecular structure characteristic of these compounds. It can also be used successfully to estimate the RI for new compounds or for other compounds whose experimental values are unknown.

## REFERENCES

1. Vagionas, K.; Ngassapa, O.; Runyoro, D.; Graikou, K.; Gortzi, O.; Chinou, I.; *Food Chem.* **2007**, *105*, 1711.
2. Kim, N. S.; Lee, D. D.; *J. Chromatogr. A* **2002**, *982*, 31.
3. Eminagaoglu, O.; Tepe, B.; Yumrutas, O.; Akpulat, H. A.; Daferera, D.; Polissiou, M.; Sokmen, A.; *Food Chem.* **2007**, *100*, 339.
4. Radulović, N.; Lazarević, J.; Ristić N.; Palić R.; *Biochem. Syst. Ecol.* **2007**, *35*, 196.
5. Kotsos, M. P.; Aligiannis, N.; Mitakou, S.; *Biochem. Syst. Ecol.* **2007**, *35*, 381.
6. Peters, R.; Tonoli, D.; van Duin, M.; Mommers, J.; Mengerink, Y.; Wilbers, A. T. M.; van Benthem, R.; de Koster, Ch.; Schoenmakers, P. J.; van derWal, S.; *J. Chromatogr. A* **2008**, *1201*, 141.
7. Li, Z. G.; Lee, M. R.; Shen, D. L.; *Anal. Chim. Acta* **2006**, *576*, 43.
8. Acevedo-Martinez, J.; Escalona-Arranz, J. C.; Villar-Rojas, A.; Tellez-Palmero, F.; Perez-Roses, R.; Gonzalez, L.; Carrasco-Velaz, R.; *J. Chromatogr. A* **2006**, *1102*, 238.
9. Teodora, I.; Ovidiu, I.; *J. Mol. Design* **2002**, *1*, 94.
10. Ghasemi, J.; Saaidpour, S.; Brown, S. D.; *J. Mol. Struct.* **2007**, *805*, 27.
11. Qin, L. T.; Liu, Sh. Sh.; Liu, H. L.; Tong, J.; *J. Chromatogr. A* **2009**, *1216*, 5302.
12. Riahi, S.; Pourbasheer, E.; Ganjali, M. R.; Norouzi, P.; *J. Hazard. Mater.* **2009**, *166*, 853.
13. Bombarda, I.; Dupuy, N.; Le Van Da, J. P.; Gaydou, E. M.; *Anal. Chim. Acta* **2008**, *613*, 31.
14. Deeb, O.; Hemmateenejad, B.; Jaber, A.; Garduno-Juarez, R.; Miri, R.; *Chemosphere* **2007**, *67*, 2122.
15. Hemmateenejad, B.; Miri, R.; Akhond, M.; Shamsipur, M.; *Chemom. Intell. Lab. Syst.* **2002**, *64*, 91.
16. Kim, K.; Lee, J. M.; Lee, I. B.; *Chemom. Intell. Lab. Syst.* **2005**, *79*, 22.
17. Rosipal, R.; Trejo, L. J.; *J. Mach. Learning Res.* **2001**, *2*, 97.
18. Haykin, S.; *Neural Networks*, Prentice-Hall: New Jersey, 1999.
19. Conforti, F.; Menichini, F.; Formisano, C.; Rigano, D.; Senatore, F.; Arnold, N. A.; Piozzi, F.; *Food Chem.* **2009**, *116*, 898.
20. Todeschini, R.; Consonni, V.; Mauri, A.; Pavan, M.; *DRAGON-Software for the calculation of molecular descriptors*; Version 3.0 for Windows, 2003.
21. Cai, W.; Xia, B.; Shao, X.; Guo, Q.; Maigret, B.; Pan, Z.; *J. Mol. Struct.* **2001**, *535*, 115.
22. Goldberg, D. E.; *Genetic Algorithms in Search, Optimization and Machine Learning*, Addison-Wesley–Longman: Reading, 2000.
23. Depczynski, U.; Frost, V. J.; Molt, K.; *Anal. Chim. Acta* **2000**, *420*, 217.
24. Citra, M.; *Chemosphere* **1999**, *38*, 191.
25. Hemmateenejad, B.; Shamsipur, M.; Miri, R.; Elyasi, M.; Foroghnia, F.; Sharghi, H.; *Anal. Chim. Acta* **2008**, *610*, 25.
26. Wold, S.; Sjostrom, M.; Eriksson, L.; *Chemom. Intell. Lab. Syst.* **2001**, *58*, 109.
27. Tang, K.; Li, T.; *Anal. Chim. Acta* **2003**, *476*, 85.
28. Rosipal, R.; Trejo, L. J.; *J. Mach. Learning Res.* **2001**, *2*, 97.
29. Zupan, J.; Gasteiger, J.; *Neural Network in Chemistry and Drug Design*, Wiley–VCH: Weinheim, 1999.
30. Beal, T. M.; Hagan, H. B.; Demuth, M.; *Neural Network Design*, PWS: Boston, 1996.
31. Zupan, J.; Gasteiger, J.; *Neural Networks for Chemists: An Introduction*, VCH: Weinheim, 1993.
32. Guven, A.; Kara, S.; *Exp. Sys. Appli.* **2006**, *31*, 199.
33. Salvi, M.; Dazzi, D.; Pelistri, I.; Neri, F.; Wall, J. R.; *Ophthalmology* **2002**, *109*, 1703.
34. Kim, K.; Lee, J. M.; Lee, I. B.; *Chemom. Intell. Lab. Syst.* **2005**, *79*, 22.
35. Booth, T. D.; Azzaoui, K.; Wainer, I. W.; *Anal. Chem.* **1997**, *69*, 3879.
36. Yu, X.; Yi, B.; Liu, F.; Wang, X.; *React. Funct. Polym.* **2008**, *68*, 1557.
37. Karelson, M.; *Molecular descriptors in QSAR/QSPR*, Wiley-Interscience: New York, 2000.
38. Todeschini, R.; Consonni, V.; *Handbook of molecular descriptors*, Wiley-VCH: Weinheim, 2000.
39. Hemmateenejad, B.; Javandnia, K.; Elyasi, M.; *Anal. Chim. Acta* **2007**, *592*, 72.
40. Golbraikh, A.; Tropsha, A.; *J. Mol. Graph. Model.* **2002**, *20*, 269.